Texture and Structure Sensitive 3D Multi-scale Deep Neural Network for MR Images Denoising

A. Aaisha Nazleem

Research Scholar, Reg No (17233152162001) S.T. Hindu College, affiliated to Manonmaniam sundaranar university, Nagarcoil .

Dr. S. S. Sujatha

Associate Professor, Department of Computer Science S.T. Hindu College, affiliated to Manonmaniam sundaranar university, Nagarcoil

ucknow

Abstract

Image denoising is a basic problem in image processing, with the aim of approximating the original image by suppressing noise in the noised image. The major objective of noise reduction is to reduce noise in natural images while preserving original characteristics and increasing signal-to-noise ratio (SNR). This paper presents a novel approach for Denoising MRI images using a variant of Generative Adversarial Network (GAN), which is named as Texture and Structure Sensitive 3D Multi-scale Deep Neural Network (TS-3D-MDNN). A revised multi scale 3D CNN model is presented as the Generator of this GAN framework in order to preserve more information. The noise is reduced by the use of Generator and a Discriminator circuit with the help of structure and texture sensitive loss model. The experimental findings reveal that the suggested technique outperforms each method individually in terms of mean square error and peak signal-to-noise ratio. The proposed TS-3D-MDNN method achieves up to 46% of PSNR.

Introduction

Magnetic Resonance Imaging (MRI)[1], a leading medical imaging technology that gives the highly comprehensive information about the human living organs and tissues including pathological and physiological changes through imaging. The MRI images provide a two-dimensional segment of the body with appropriate tissue location, contrast, and orientation. High-resolution MR images with a high signal-to-noise ratio (SNR) allow for more detailed imaging of anatomical features, boosting predictive accuracy and aiding early-stage diagnose of a variety of central nervous system illnesses.[2-4]. Increasing the number of image acquisitions (NAQ), altering the acquisition bandwidth, and utilising high magnetic field intensity, are some of the methods for obtaining high-resolution MR pictures with high-SNR. At the same time, increasing NAQ takes longer acquisition time. Images with low SNR will be aesthetically corrupted and will have noise added to them. The efficiency of MRI decreases when a region or specific tissue affects from a low signal to noise ratio (SNR).As a result, an efficient MRI reconstruction procedure is required, in which denoising algorithms are used to noisy images to enhance both qualitative and quantitative MRI metrics.

Image Denoising is an essential step for MR image pre-processing in several applications since it is a basic image processing issue. Images become prone to the development of certain random noise during picture capture due to intrinsic physical restrictions of various recording equipment. Noise is a fundamental signal distortion that obstructs the observation and extraction of information from images. Image noise suppression is a fundamental component of image analysis and processing, therefore any improvement in the picture denoising area aids our comprehension of fundamental image statistics and processing. Denoising methods can be applied to pictures during, or after they have been acquired. After post-acquisition denoising, the goal is to lower the strength of noise while keeping the original image's resolution.

Several denoising methods exist, like spatial filtering [5], sparse representation [6], frequency domain filtering [7] and so on. Furthermore, several neural network architectures have been developed for denoising problems including auto-encoder, CNN etc. However, there are several issues that require on-going research, such as texture restoration, detail preservation and spatial noise reduction. This present work utilised a variant of Generative Adversarial Network (GAN), which utilises an adversarial loss to compel generated images to be as similar to real images as possible, has shown excellent results in image reconstruction tasks. The proposed approach has been employed to overcome the gaps in denoising MRI images by GAN network with incorporate structural loss and textural loss.

2. Related Work

Traditional MRI denoising approaches are usually based on filtering, transformations, or statistical methods to increase performance while lowering computing time and cost.[8-10]. Gabinger-Rose [11] et al proposed an approach for removing noise using bilateral filter and Gaussian scale mixtures from digital images. Tomasi and Manduchi[12] proposed a non-iterative edge-preserving bilateral filter. It utilises a low-pass denoising kernel to adjust to the original picture's spatial distribution of pixel values when applied to an image. While denoising the image, this helps to keep the edges intact. Benesty [13] develops a novel Wiener filter for noise reduction which is based on the variance and pseudo-variance of the short time. It improves the signal-to-noise ratio (SNR). Mohan et al [14] proposed Neutrosophic Wiener Filtering approach for removing Rician noise from magnetic resonance image.

Wavelet transform, Fourier transform, Curvelet, Threshold function, and Contourlet, are used in transform domain filtering. Soft thresholding and Hard thresholding are two types of thresholding functions proposed by Donoho and Johnstone [15, 16]. Discontinuity is the drawback of hard thresholding, whereas soft thresholding has the disadvantage of causing continual divergence [17]. Based on image decomposition using Morphological Component Analysis, Zeng et al [18] presented a strategy to eliminate Gaussian noise in MR brain images (MCA).

To decrease noise in the texture, cartoon, and residual sections, wavelet hard threshold, wavelet soft threshold (classical transform domain filtering), and the Wiener filter (classical spatial domain filtering) are used. Naveed et al [19] proposed a new signal denoising method that employs the Cramer Von Misses (CVM) statistic locally on multiscale signal decomposition produced from VMD. The acquired CVM values (at several scales) are tested whether they conform to noise distribution using a nonlinear thresholding strategy based on the Goodness of Fit (GoF) test. The sections of the signal that are consistent with noise are removed, while the remainder is kept. The Markov random field (MRF) based approaches that work in the spatial domain and detect the inter-relationship between pixels have been developed by [20][21]. It preserves the edges and structures of an image, which aids in noise regulation and smoothing of image signals depending on local features.

Wang et al. [22] developed a fusion image denoising filter to take away the additive white Gaussian noise. The fusion of total variation (TV) and curvelet transform method are used to create this filter. When compared to algorithms that exclusively use the curvelet transform, the hybrid filter provides greater visual excellence.

3D filtering, and Block-matching sometimes known as "BM3D", is at the heart of the new denoising process was introduced by [23]. The goal of this BM3D algorithm is to increase the sparse representation of a transform domain [24]. Yahya et al[25] introduced a new BM3D image denoising technique based on k-means clustering and Adaptive filtering. Initially, an adaptive filtering function is used to replace the BM3D filter's typical hard thresholding. Following that, an adaptive threshold is used to apply the proposed adaptive filtering function. By utilising k-means clustering, the block matching is forced to search inside the region of the reference patch, reducing the chance of bad matching.

Recently, Deep learning has found to be a very efficient technique in the field of medical imaging. CNN-based denoising approaches target to learn a mapping function by optimising a loss function on a training set of degraded-clean picture pairings [26,27].To keep the advancement in extremely deep architecture, learning algorithm, and regularisation approach into image denoising, Zhang et al [28] created feed-forward denoising convolutional neural networks (DnCNNs).To increase the speed of the training process and increase the denoising performance, residual learning and batch normalisation are used. Moreover, zheng et al [29] proposed a fast and flexible denoising convolutional neural network (FFDNet) with an adjustable noise level map as the input. This new FFDNet approach operates on down sampled sub images and achieves a good balance of denoising performance and inference speed.

Several studies [30-31] have been started to work with losses. The effect of denoising is captured by perceptual loss [32], which finds the difference between the reference image and the denoised image. However, because the evaluation is done in generic ways, perceptual loss-based work does not work well when applied to conventional images. Different types of Generative Adversarial Networks (GAN) were employed to overcome this issue. By evaluating structural sensitivity of the pictures, Chenyuet et al [33] employed a Multi-scale Generative Adversarial Network (SMGAN).For picture denoising, ZhiPing et al. [34] suggested a novel generative adversarial network (GAN). To represent the distance between the data distribution of clean and denoised pictures, the whole network is trained using a new textural loss. Several approaches have been described for denoising MR Images with structured loss and textured loss. Even though the denoising methods available in literature are accepted, still there is a need to reported performance to a satisfactory level. The proposed approach has been employed to overcome the gaps in denoising MRI images by GAN network with incorporate structural loss and textural loss.

3. Proposed Work

In this proposed work, Reformed Structural Loss based 3D Multi-scale Deep Neural Network has been modified with GAN network. The proposed network, which is based on SMGAN [33], gives structurally-sensitive loss that impacts three types of losses:

perceptually-favourable structural loss, pixel-wise L1 loss, and adversarial loss.

The main goal of denoising is to remove the desired image x from a noisy image y. Figure1 illustrate the complete map of the proposed architecture. It is composed of four components: a generator, Textural Loss (TL) functions, Structurally Sensitive Loss (SSl) functions and discriminator. The 3D multi-scale CNN Generator G is used to convert the noisy MRI image into a noise-free MRI image. The Textural Loss is used to reduce the noise. The difference in structural sensitiveness between both images is calculated by SSL. The Discriminator D is used to distinguish between synthetic and actual findings. They compete with each other to improve the results based on the outcomes of G and D. The functionality of Generator, Textural Loss, Structurally sensitive loss, and Discriminator are discussed elaborately in the following sections.

Figure 1. Complete Map of Proposed Architecture

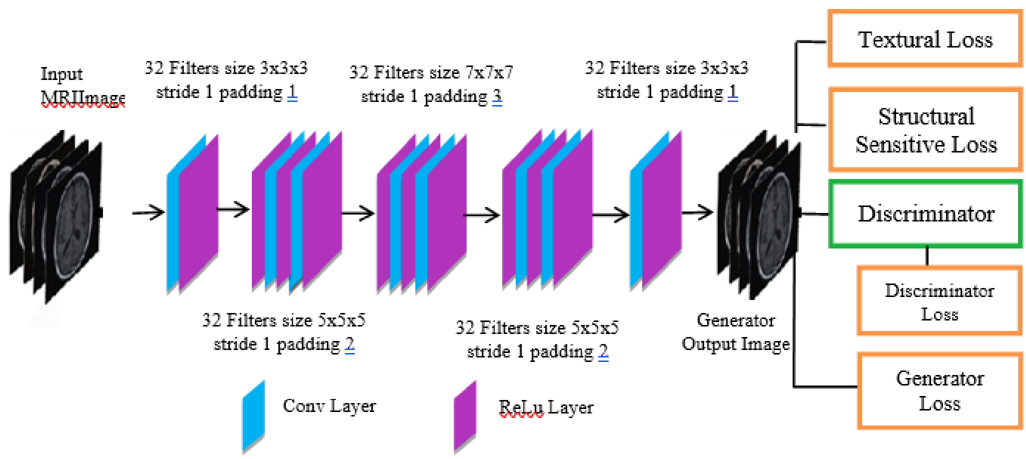

3.1 3D Multi Scale CNN Generator

A reformed model of multi scale 3D CNN model is offered as the Generator of this GAN framework in order to preserve more textural and structural information. The Generator G is utilised for synthesizing the new data from previously accessible data. It also helps to reduce image noises in the feature domain. The generator with layers is used in the proposed network. Each layer has 32 filters. There are five levels in all. The first level which contains one convolutional layer, has 3x3x3 filters with padding of one. The second level consists of three convolutional layers, and it has 5x5x5 filters with padding two. The third level, which includes three convolutional layers, has 7x7x7 filters with padding 3. The fourth convolutional layer consists of 5x5x5 filters with padding of 2. The final convolutional layer has 3x3x3 filters with padding of 1. The Rectified Linear Unit (ReLU) operation is applied following each convolutional operation.

3.2 Discriminator

The Discriminator D network used in this work does its best to differentiate the denoised images from clean images. The discriminator network does its best to discriminate between denoised and clean images. The discriminator produces a probability that represents the resemblance between the denoised and clean image. Discriminator network consists of six convolutional layers with the filter sizes of 64, 64, 128, 128, 256, and 256 with a kernel size 3x3x3. Two fully connected (FC) layers are employed after the convolutional layers that produce 1024 and 1 feature maps respectively. Following each fully connected with ReLU layer.

3.3 Textural Loss

3.3.1 Texture Extraction

Any image I is decomposed into a cartoon component, c, where just the image contrasting shapes appear, and a textural part t with oscillating patterns through the cartoon-texture algorithm. The decomposition I = c + t is equivalent to the low pass and high pass filter decomposition used in signal processing. Though, the cartoon portion of an image, comprises strong edges and hence all frequencies, up to and including the highest, but a texture can also contain intermediate and high frequencies.

The key characteristic of a textured region of an image is its high total variation. Two low pass filters are applied to compute the Gradient image from the original image, which are performed directly by a discrete convolution. The simplest centred difference approach is used to calculate the gradient. The key steps are:

1. Initially a low pass filter is applied to the original image I.

Convoluting original image I with the low pass filter L_σ =(Id-(Id-G_σ)n) yields the low pass filtered image 〖L〗_σ *I. Where G_σ is a Gaussian kernel with standard deviation σ and n denoting that the convolution is repeated n times and n set to 5.The image is symmetrised out of its domain while convolutions are generated in space with mirror boundary conditions. This low pass filtered image is produced iteratively in the current application.

2. Calculate the Euclidian norm of the image gradients of I and $L_\sigma * I$

A centred two-point technique is used to calculate the vertical and horizontal derivatives, as well as the modulus of the gradient using a Euclidean norm.

$$p_x(i,j) = p(i+1,j) - p(i-1,j) \quad (1)$$

$$p_y(i,j) = p(i,j+1) - p(i,j-1) \quad (2)$$

$$|\nabla p| = \sqrt{p_x(i,j)^2 + p_y(i,j)^2} \quad (3)$$

3. Calculate the local total variation of I and $L_\sigma * I$, by combine these moduli with the Gaussian G_σ . Convolutions are calculated using mirror boundary conditions in space.
4. Determine the value of λ(x) at every point in the image.
5. Determine the value of the cartoon image by taking the weighted average of I and $L_\sigma * I$.
6. Compute the texture as the difference $p - I$.

3.4 Structurally Sensitive Loss

A structurally sensitive loss (SSL) function is used to enhance the accuracy and robustness of the algorithm, which measures the dissimilarities in patch-wise. In this study, the 3D SSL function is employed to differentiate between 3D output from the multi-scale convolutional network and 3D NFMRI images. This data is used to update network parameters.

Structurally-Sensitive Loss (SSL) SSL function [32] is used to find the differences in patch-wise. 3D SSL function is used in this work the difference of 3D output and 3D NFMRI image. This information is used for updating network parameter.

The structural loss is calculated by using C1 and C2 which are constants. μ_x, μ_z, σ_x, σ_z and σ_{xz} denote the mean of image x, mean of image z, standard deviation of x, standard deviation of z and cross-covariance of the images x and z. x is the image and z is the corresponding NFMRI image. The structural similarity index (SSIM) can be calculated using Equation.1

$$SSIM(x,y)=\frac{2\mu_x\mu_z+C_1}{\mu_x^2+\mu_z^2+C_1} * \frac{2\sigma_{xz}+C_2}{\sigma_x^2+\sigma_z^2+C_2} = l(x,z) * cs(x,z). \quad (4)$$

From the SSIM measure, we can calculate multi-scale structural similarity index (MS-SSIM) as $MS-SSIM(x,z) = \prod_{i=1}^{M} SSIM(x_i, z_i)$. From these data, SSL can be calculated as $ss_L = 1 - MS - SSIM(x,z)$ Let x and y be the noise free MRI (NFMRI) image and noisy MRI image (NMRI) respectively with W, H, and D where W is width, H is height, and D is number of slices. The relationship between these images is represented by 5:

$$y = T(x) + \varepsilon \quad (5)$$

Where T is a generic noising process which degrades the image. H, W and D are height, width and depth respectively. The aim of denoising is to extract the desired image x from the noisy image y. This can be done by solving inverse problem as T^t=T^(-1) which will help to retrieve the denoised image. The output will be T^t y≃ẍ≃x. Figure 1 gives the proposed architecture. It has four parts: a generator, Structurally-Sensitive loss (SSL) function, Texture Sensitive Loss and discriminator. The noisy MRI image is converted into noise free MRI image using G. The dissimilarity in structural sensitiveness between both is calculated by SSL. D is used to differentiate the synthetic results from real one. Based on the outcome of G and D, they compete each other in improving the results. The following part of this section describes about the structure and functionality of G, SSL and D.

3.5 Generator Loss

Generator loss is a balancing technique for sustaining natural internal statistics [36]. This loss trains a feed-forward CNN to maintain natural interior information. Generator loss function represents the difference value attained from the generated denoised image and actual image as represented in Eq. (6) and Eq. (7).

$$gen_L = \|u - \hat{u}\|_1 \quad (6)$$

$$gen_L = E_{u\sim pu} \|u - G(u)\|_1 \quad (7)$$

Here, u represents actual image and uˆ represents the generated image

3.6 Discriminator Loss

Discriminator loss maximizes the average of the log probability for actual image and the log of the inverted probabilities of fake image. Discriminator loss function represents the difference value between the generated image obtained from the generator and actual image by applying discriminator network. The output of the generator is passed to estimate actual or fraud using functionf as shown in the eq. (8).

$$dis_L = \|f(u) - f(\hat{u})\|_2 \quad (8)$$

An objective function of this model is calculated by combining Generator loss (gen_L), Discriminator Loss(dis_L) and Texture loss ($text_L$),Structurally sensitive loss(ss_L) .Overall, the loss estimated using GAN network is obtained using Eq. (9).

$$FINAL_{LOSS} = gen_L gen_W + dis_L dis_W + text_L text_W + ss_L ss_W + \quad (9)$$

Where gen_W, dis_W , text_W , ss_W are the weighting values for each loss. Where $\text{gen}_W = 0.3$, $\text{dis}_W = 0.3$, $\text{text}_W = 0.2$ and $\text{ss}_L = 0.2$.

4. Experimental Analysis

4.1 Dataset

The effectiveness of the proposed work is evaluated by BraTS'17 dataset. Glioblastoma (GBM/HGG) and lower grade glioma (LGG) multimodal MRI scans with pathologically confirmed diagnosis are used as training, validation, and testing data. From the BraTS'17 dataset, T1cMRI brain DICOM image of 20 individuals are employed for this study. There are 154 slices in each patient group. In this study, 70% of the images are chosen at random for the training set, while the remaining 30% are utilised for the testing set.

4.2 Performance Metrics

Three image quality assessment measures such as Peak signal-to-noise ratio (PSNR), Structural Similarity Index Measure (SSIM) and Normalized Cross-correlation (NCC) are utilised to evaluate the performance of the proposed method.

Peak signal-to-noise ratio (PSNR) compares two images. This ratio compares the quality of the denoised image to that of the original image.

PSNR can be determined using Equation 10.

$$PSNR = 10 \log_{10} \left(\frac{MAX^2}{MSE} \right) \qquad (10)$$

where MAX indicates the Maximum Intensity Value of the image, while the Mean Square Error is MSE.

The Structural Similarity Index Measure (SSIM) is a technique for determining the perceived difference between two similar pictures. SSIM index between the two images with same size $N \times N$ can be calculated using Equation 11.

$$SSIM(x, y) = \frac{(2\mu_x \mu_y + c_1)(2\sigma_{xy} + c_2)}{(\mu_x^2 + \mu_y^1 + c_1)(\sigma_x^2 + \sigma_y^2 + c_2)} \qquad (11)$$

Normalized Cross-correlation (NCC) metrics is often used to assess the degree of similarity (or dissimilarity) between two similar images. This can be calculated using Equation12.

$$\text{NCC}(\text{Image1}, \text{Image2}) = \frac{1}{N\sigma_1\sigma_2} \sum_{x,y} (\text{Image1}(x, y) - \overline{\text{Image1}}) x (\text{Image2}(x, y) - \overline{\text{Image2}}) \qquad (12)$$

Where N is the total number of pixels in the image, σ_1 and σ_2 are standard deviation values. Image 1 and Image 2 are NFMRI and NMRI.

4.3 Result and Analysis

The following

Table 4.1 shows the denoised image by the proposed TS-3D-MDNN.

Input Noise Image	De-noised Image	PSNR
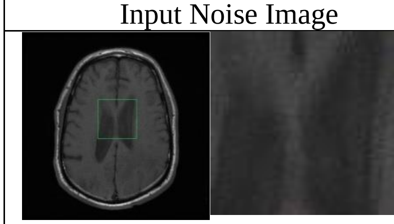	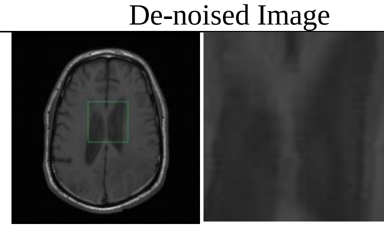	46.32

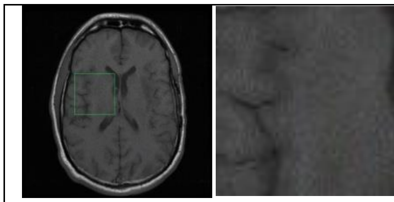	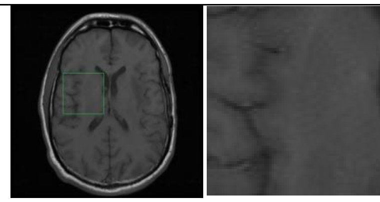	45.26
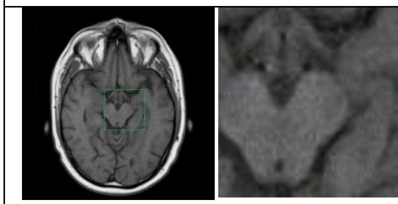	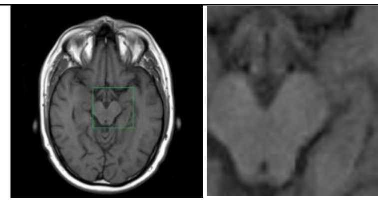	46.58
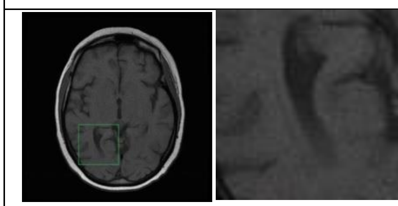	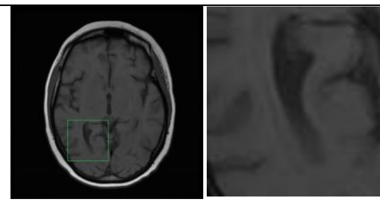	45.73

Table.4.2 Performance of TS-3D-MDNN, SMGAN-3D, WGAN, CNN_L1 and RSLM-DNN-3D based on the PSNR value for the slice of T1 weighted MRI DICOM images.

PatientID	1	2	3	4	5	6	Mean
CNN_L1	37.56	38.27	37.94	36.72	37.09	37.61	37.53167
WGAN	40.78	37.45	39.02	38.69	40.01	40.59	39.42333
SMGAN-3D	42.82	39.03	41.8	40.47	41.55	41.63	41.21667
RSLM-DNN-3D	44.51	44.96	44.55	43.76	43.73	43.96	44.245
TS-3D-MDNN	46.65	46.98	46.8	44.86	45.83	44.26	45.89667

Figure4.1: Comparison of PSNR value for the slice of T1 weighted MRI DICOM images of proposed work with previous works

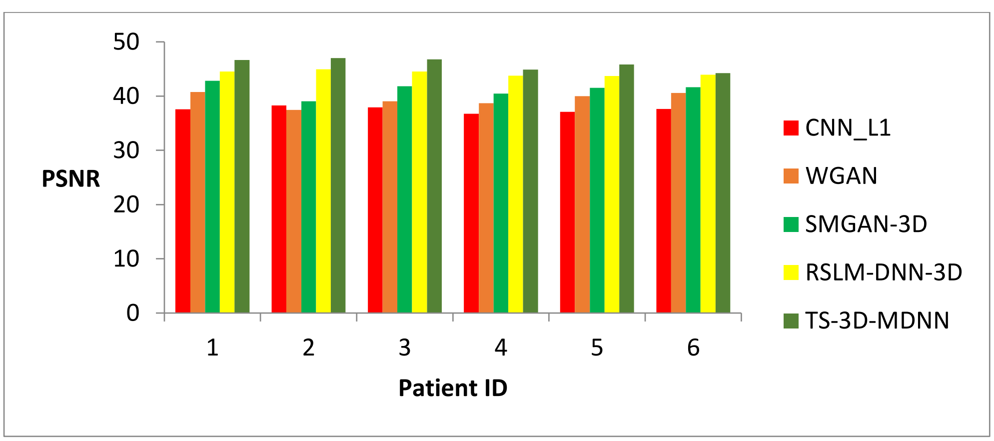

From these it is clear that the proposed work outperforms other previous works. The method CNN_L1 has PSNR values 37.53%,WGAN Has 39.42%,SMGAN-3D has 41.21%,RSLM-DNN-3D has 44.24% and TS-3D-MDNN has 45.89%. Here, the TS-3D-MDNN method attained PSNR score better than the remaining methods. PSNR value of the TS-3D-MDNN method is 1.65% higher than theRSLM-DNN-3D method. RSLM-DNN-3D is 3.03% higher than the method SMGAN-3D. SMGAN-3D is 1.79%higher than the method WGAN. WGAN is 1.89% higher than the method CNN_L1.

Table4.3 shows that the performance of TS-3D-MDNN,SMGAN-3D,WGAN,CNN_L1 and RSLM-DNN-3D based on the SSIM value for the slice of T1 weighted MRI DICOM images and Figure4.2 gives the diagrammatic representation of the same. From these it is clear that the proposed work outperforms than the previous works.

Table.4.3 Performance analysis of TS-3D-MDNN, SMGAN-3D, WGAN, CNN_L1 and RSLM-DNN-3D based on the SSIM value for the slice of T1 weighted MRI DICOM images.

PatientID	1	2	3	4	5	6	Mean
CNN_L1	0.967	0.9601	0.95	0.944	0.94	0.954	0.952517
WGAN	0.9694	0.967	0.9622	0.9532	0.9452	0.9595	0.959417
SMGAN-3D	0.9802	0.97865	0.97662	0.964	0.962	0.9765	0.972995
RSLM-DNN-3D	0.99	0.9902	0.9899	0.983	0.984	0.98934	0.98774
TS-3D-MDNN	0.994	0.993	0.992	0.986	0.989	0.995	0.9915

Figure 4.2: Comparison of SSIM values for the slice of T1 weighted MRI DICOM images of various works

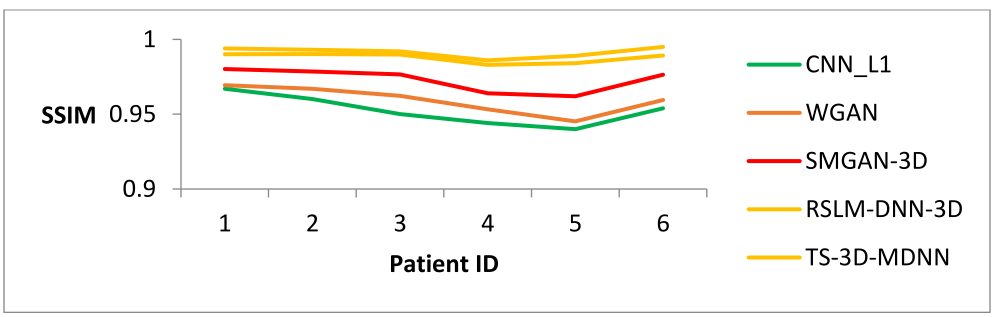

The method CNN_L1 has PSNR values 0.9525%, WGAN has 0.9594%, SMGAN-3D has 0.9729%, RSLM-DNN-3D has 0.9877% and TS-3D-MDNN has 0.9915%. Here, the TS-3D-MDNN method attained SSIM score better than the remaining methods. SSIM value of the TS-3D-MDNN method is 0.0038% higher than theRSLM-DNN-3D method. RSLM-DNN-3D is 0.0148% higher than the method SMGAN-3D. SMGAN-3D is 0.0135% higher than the method WGAN. WGAN is 0.0069% higher than the method CNN_L1. The following Table.4.3 shows that the performance of SMGAN-3D, WGAN, CNN_L1 and RSLM-DNN-3D based on the NCC value for the slice of T1 weighted MRI

DICOM images and Figure 4.3 gives the diagrammatic representation of the same which show the better performance of the proposed work when compared to the other previous works

Table.4.4 Performance of TS-3D-MDNN, SMGAN-3D, WGAN, CNN_L1 and RSLM-DNN-3D based on the NCC value for the slice of T1 weighted MRI DICOM images.

PatientID	1	2	3	4	5	6	Mean
CNN_L1	0.961	0.9574	0.9491	0.9545	0.939	0.9536	0.952433
WGAN	0.963	0.97633	0.9652	0.9633	0.9433	0.9599	0.961838
SMGAN-3D	0.974	0.98934	0.9734	0.9688	0.9688	0.9733	0.974607
RSLM-DNN-3D	0.988	0.993	0.989	0.9878	0.978	0.982	0.9863
TS-3D-MDNN	0.991	0.995	0.993	0.988	0.982	0.989	0.989667

Fig. 4.3. Performance comparison of NCC of SMGAN-3D, WGAN, CNN_L1 and RSLM-DNN-3D.

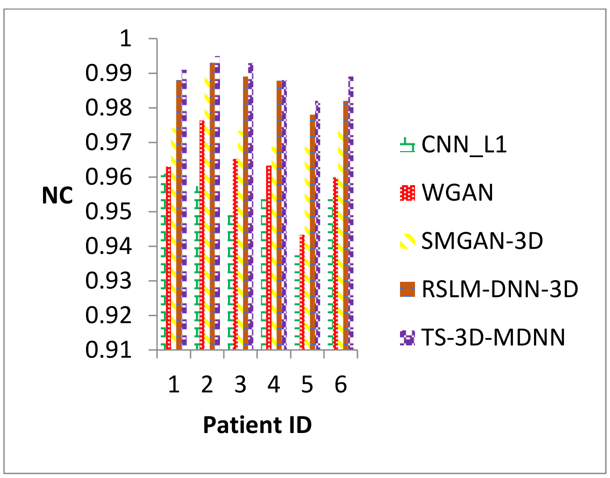

The method CNN_L1 has PSNR values 0.9524%, WGAN has 0.9618%, SMGAN-3D has 0.9746%, RSLM-DNN-3D has 0.9863% and TS-3D-MDNN has 0.9896%. Here, the TS-3D-MDNN method attained PSNR score better than the remaining methods. PSNR value of the TS-3D-MDNN method is 0.0033% higher than the RSLM-DNN-3D method. RSLM-DNN-3D is 0.0117% higher than the method SMGAN-3D. SMGAN-3D is 0.0128% higher than the method WGAN.WGAN is 0.0094% higher than the method CNN_L1. The structural and textural sensitiveness of the images gives better information to work on with various losses. Hence the proposed approach achieves significant improvement in performance metrics.

5. Conclusion

This paper proposes a Generative Adversarial Network (GAN) model for denoising the MRI images. TS-3D-MDNN Multi Scale Deep Neural Network model is designed with two effective loss functions to enhance the performance of denoising in medical image sequence especially MRI images. In order to preserve the sensitive information a revised 3D Multi Scale CNN is designed in this work. This denoising model is aware of texture and structure data and preserves those data at that time of denoising process. The structural loss is estimated with the help of multi scale structural similarity index where as textural loss is calculated with the help of cartoon decomposition approach. The proposed GAN with Texture and Structure Sensitive 3D Multi-scale Deep Neural Network TS-3D-MDNN achieves up to 46% of PSNR.

Reference

Wright G, (1997). “Magnetic Resonance Imaging”, IEEE Signal Process Mag. 14, pp.56-66.

MalmgrenK,&Thom M. (2012). “Hippocampal sclerosis—origins and imaging”,Epilepsia53, pp.19–33.

Jonkman LE, Klaver R, Fleysher L, IngleseM&Geurts JJ. (2015). “Ultra-high-field MRI visualization of cortical multiple sclerosis lesions with T2 and T2 *: a postmortem MRI and histopathology study”, AJNR Am J Neuroradiol, 36, pp. 2062–2067.

Thom M. Review: Hippocampal sclerosis in epilepsy: a neuropathology review. NeuropatholApplNeurobiol 2014; 40:520–543.

Liu X, Huang L, &Guo Z. (2011). “Adaptive Fourth-Order Partial Differential Equation Filter for Image Denoising”. Applied Mathematics Letters, 24(8), pp. 1282-1288.

Chen G,&Qian S E. (2011). “Denoising of Hyperspectral Imagery Using Principal Component Analysis and Wavelet Shrinkage”, IEEE Transactions on Geoscience & Remote Sensing, 49(3),pp. 973-980.

Sendur, L,&Selesnick IW. (2002).“Bivariate Shrinkage Functions for WaveletBasedDenoising Exploiting Interscale Dependency”. Signal Processing IEEE Transactions on, 50(11), pp.2744-2756.

Erturk M. (2013). “De-noising MRI using spectral subtraction”. IEEE Transaction on Bio-Medical Engineering. 60(6).

Patel K,&Mewada H. (2014). “A review on different image de-noising methods. International Journal on Recent and Innovation Trends in Computing and Communication”. 2(1), pp.155-159.

Bourne R. (2010). “Image filters. In: Fundamentals of Digital Imaging in Medicine”, Springer London;

Gabiger-Rose, A, Kube, M, Schmitt, P, Weigel, R, & Rose, R. (2011). "Image denoising using bilateral filter with noise-adaptive parameter tuning," IECON 2011 - 37th Annual Conference of the IEEE Industrial Electronics Society, pp. 4515-4520, doi: 10.1109/IECON.2011.6120053.

Tomasi, C, &Manduchi, R. (1998). “Bilateral Filtering for gray and Color Images,” in Proceedings of the Sixth International Conference on Computer Vision (IEEE Computer Society), ICCV ’98), 839.

Benesty J, Chen JD, &Huang YT (2010),“Study of the widely linear wiener filter for noise reduction”. Abstracts of IEEE international conference on acoustics, speech and signal processing, pp.205–208. doi:10.1109/ICASSP.2010.5496033

Mohan J, Krishnaveni V, Guo Y &Kanchana J, (2012). “MRI denoising based on neutrosophic wiener filtering”, Proc. IEEE International Conference on Imaging Systems and Techniques (IST 2012) Manchester, United Kingdom.

DonohoD. L &Johnstone, I.M (1994), “Ideal spatial adaptation BY wavelet shrinkage,” Biometrika, 81(3), pp. 425–455.

Donoho D.L., (1995), “De-noising by soft-thresholding,” IEEE Transactions on Information Theory, 41(3), pp. 613– 627.

Zhang, Y., Ding, W., Pan, Z., & Qin, J. (2019). Improved Wavelet Threshold for Image De-noising. Frontiers in neuroscience, 13, 39. Doi:10.3389/fnins.2019.00039

Zeng, Y., Zhang,B., Zhao, W., Xiao, S., Zhang,, G., Ren, H., Zhao, W., Peng,Y., Xiao, Y., Lu, Y., Zong, Y., & Ding, Y., (2020), "Magnetic Resonance Image Denoising Algorithm Based on Cartoon, Texture, and Residual Parts", Computational Intelligence Methods for Brain-Machine Interfacing or Brain-Computer Interfacing. doi:10.1155/2020/1405647

Naveed, K., Akhtar,M.T., Siddiqui, M,F., &Rehman, N.,(2020), A statistical approach to signal denoising based on data-driven multiscale representation, Digital Signal Processing, 108, https://doi.org/10.1016/j.dsp.2020.102896.

Baselice F, Ferraioli G, &Pascazio V. (2016), "A Bayesian approach for relaxation times estimation in MRI", MagnReson Imaging. 34(3),312–25

Descombes X, Kruggel F, &von Cramon DY. (1998), "fMRI signal restoration using a spatio-temporal markov random fieldpreserving transitions". NeuroImage. 8(4),pp. 340–9.

Wang HZ, Qian LY, &Zhao JT (2010) An image denoising method based on fast discrete curvelet transform and total variation. In:Proceedings of the IEEE international conference on software processing, pp 1040–1043

Dabov K, Foi A, Katkovnik V, &Egiazarian K (2007) Image denoising by sparse 3-D transform-domain collaborative filtering. IEEE Trans Image Process 16(8): 2080–2095. https://doi.org/10.1109/TIP.2007.901238.

Naveen S, &Aiswarya VA (2015) Image denoising by Fourier block processing and Wiener filtering. Procedia Computer Science 58, 683–690

Yahya, A.A., Tan, J., Su, B. et al. BM3D image denoising algorithm based on an adaptive filtering. Multimed Tools Appl, 79, pp.20391–20427 (2020). doi:10.1007/s11042-020-08815-8

Chen YY, Pock T (2017) Trainable nonlinear reaction diffusion: a flexible framework for fast and effective image restoration. IEEE Trans Pattern Anal Mach Intell 39(6):1256–1272. https://doi.org/10.1109/TPAMI.2016.2596743

Schmidt U, Roth S (2014) Shrinkage fields for effective image restoration. In: Abstracts of 2014 IEEE conference on computer vision and pattern recognition. IEEE, Columbus, pp 2774–2781. https://doi.org/10.1109/CVPR.2014.349

Zhang K, Zuo WM, Chen YJ, Meng DY &Zhang L (2017) Beyond a Gaussian denoiser: residual learning of deep CNN for image denoising. IEEE Trans Image Process 26(7), pp. 3142–3155. doi:10.1109/TIP.2017.2662206

Zhang K, Zuo WM, Zhang L (2018) FFDNet: toward a fast and flexible solution for CNN-based image denoising. IEEE Trans Image Process 27(9): 4608–4622.doi:10.1109/TIP.2018.2839891

Wolterink, J M., Leiner, T.,Viergever, M.A.,&Iˇsgum, I, (2017), "Generative adversarial networks for noise reduction in low-dose CT," IEEE Trans.Med.Imaging, 36(12), pp. 2536–2545,

Zhao, H. Gallo, O.,Frosio, I.,&Kautz, J., (2017), "Loss functions for image restoration with neural networks," IEEE Trans. Comput.Imaging, 3(1), pp. 47–57.

Yang, Q., Yan, P., Zhang, Y, Yu, H., Shi, Y., Mou, X., Kalra, M K.,&. Wang, G (2017), "Low dose CT image denoising using a generative adversarial network with wasserstein distance and perceptual loss," arXiv preprint arXiv:1708.00961

Chenyu, Y., Qingsong, Y., Hongming, S, Lars G., Guang L, Shenghong, J, Zhuiyang Z, & Zhen (2020) " Structurally-sensitive Multi-scale Deep Neural Network for Low-Dose CT Denoising," IEEE Access, Vol.6

ZhiPing, Q.,YuanQi, Z., Yi, S.,&Xiangbo, L. (2018). A New Generative Adversarial Network for Texture Preserving Image Denoising. 1-5. 10.1109/IPTA.2018.8608126.